

CETA-F: Scintillator camera for 100kV Single Particle Analysis

Miloš Malínský¹, PhD., Gerald van Hoften², Yu Lingbo², PhD., Ondřej Vyroubal¹, Vojtěch Doležal¹, Markéta Červinková¹, PhD.

¹Thermo Fisher Scientific Brno s.r.o., Material & Structural Analysis, Brno, Czech Republic

²Thermo Fisher Scientific, Material & Structural Analysis, Eindhoven, the Netherlands

ABSTRACT

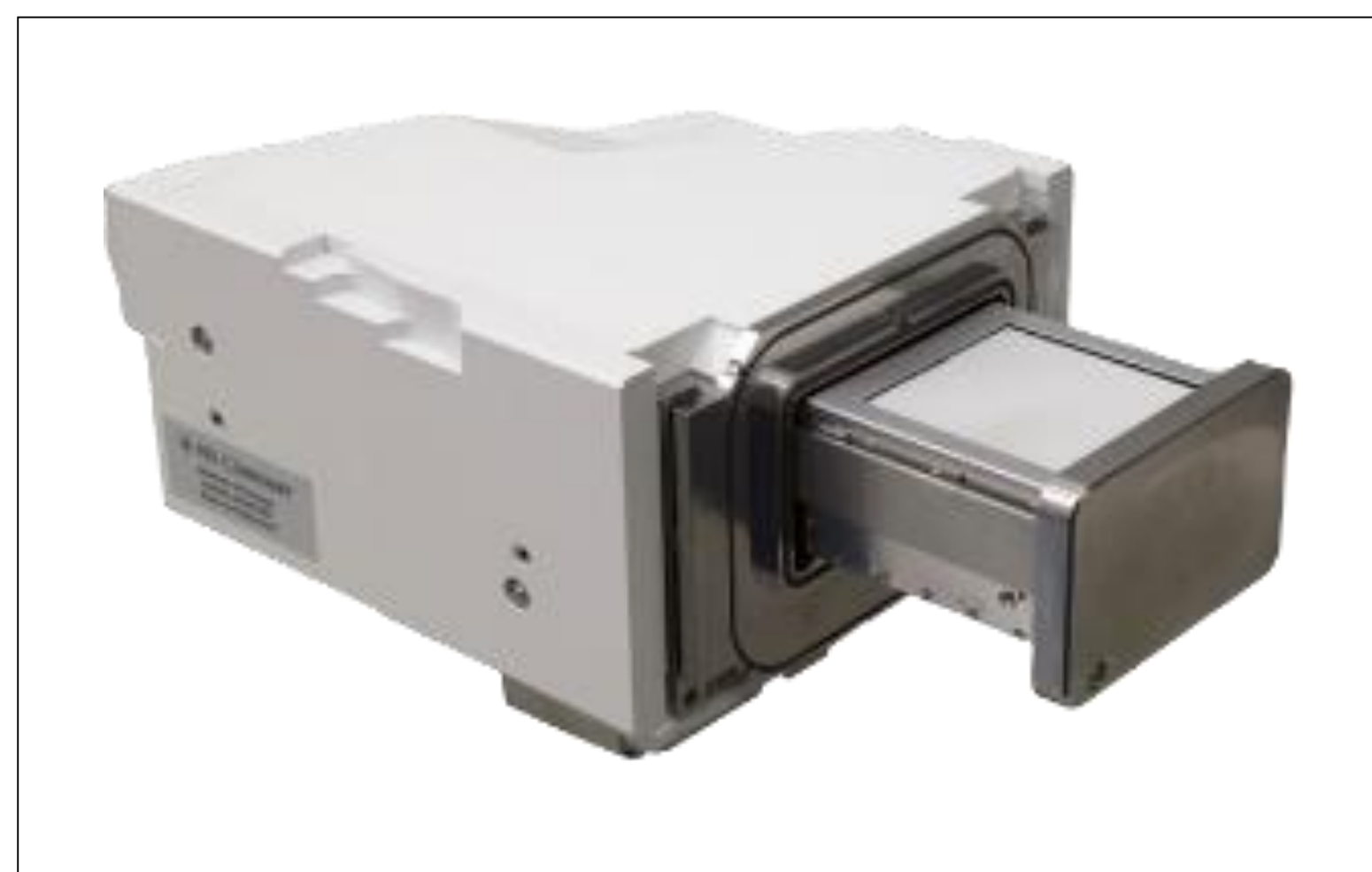
Single-Particle cryo-electron microscopy is a well-established technique which provides information about high-resolution details of biological structures. Over the last 10 years direct electron detectors (DED) became the leading technology for low-dose imaging of radiation sensitive samples; however, the technology remains out of reach for most institutions as it is rather costly. Recently, Thermo Fisher Scientific introduced the Tundra, a new Cryo-TEM that is dedicated to SPA and operates at 100kV. Our mission with the Tundra is to enable adoption of Cryo-EM SPA by the broader life sciences community, including biochemistry laboratories and users without electron microscopy background. The Tundra offers biologically-relevant performance at a more affordable price point.

In this poster, we demonstrate that a significantly more affordable scintillator-based camera with good sensitivity can substitute for expensive DED cameras at 100kV. This choice was validated not only by image quality measurements but also by repeated SPA runs of various cryo-EM samples.

INTRODUCTION

Thermo Fisher Scientific introduced Tundra cryo-EM system equipped with a scintillator based camera called CETA-F. Since Tundra is a new system in a Thermo Scientific™ cryo-EM family operating at non-standard 100kV, limited direct electron cameras are available. Majority of these cameras are dedicated for 200kV and 300kV systems e.g. Glacios™ and Krios™, respectively. DED cameras have limited performance at lower high tensions (HT) or suffer with radiation damage due to particular design of the pixel structure. As part of this poster we compare the performance of scintillator based CETA-F camera with typical DED and hybrid concept [1].

Figure 1. CETA-F camera



Lower energy (100kV) of primary electron causes larger interaction cross-section with the detection layer of the DED cameras. Current architecture of DED requires design modifications to enable high performance at 100kV. There are two possibilities how to optimize the design of DED for lower HT range. The first option is to increase the pixel size, which limits camera FOV due to volume constraints in camera block. This is typical for hybrid type of detectors. The second option is to limit the thickness of the detection active layer (back thinning of the sensor) which can be technologically challenging.

Lower HT is an advantage for CETA-F camera. The 4kx4k CETA-F camera is coupled with 1:1 fiber optics plate which includes dedicated P43 phosphor. The camera has 14µm pixel size and it is running at linear mode using correlated double sampling (CDS) with a fix frame rate of 14fps. The CDS option helps to reduce the dark noise of the camera.

MATERIALS AND METHODS

There are multiple ways how to measure and compare performance of different cameras. Since a direct electron detector dedicated for 100kV is currently not available we compare CETA-F with theoretical values of typical DED camera (based on 200kV and 300kV knowledge) and performance specifications defined for hybrid detectors around 100kV [3].

Tundra introduces the 4kx4k CETA-F camera with four times improved sensitivity at 100kV compared to the standard CETA 16M product. Importantly, at 100kV the higher sensitivity and increased photon yield density within the CETA-F scintillator layer significantly improves low dose DQE [2] as demonstrated in Figure 2. The figure shows DQE curves, where spatial frequency is normalized to the line pairs (lp) per camera field of view (FOV) to distinguish between various camera resolutions. CETA-F is a viable and inexpensive 100kV detector alternative to the more expensive DED and hybrid detectors. Moreover, it does not suffer from the low FOV and radiation hardness challenges typically associated with hybrid and 100kV DED technology, respectively. The CETA-F camera is proven to be sufficient for SPA data acquisitions as well as complete TEM optical alignments.

The CETA-F camera is equipped with dose-fractionation mode and offloading functionality that enables reconstruction of high resolution protein structures. Acquisition of dose-fractions provides option to reduce motion of the sample cause by beam induced movement and remove of the sample drift.

Since the frame rate and SNR is lower for the scintillator based cameras, the dose rate definition has to be balanced between sufficient dose per frame and number of fractions acquired. Tundra system introduced the optical preset options, which helps users to correctly set this.

DQE analysis

The well-known camera performance characterization method of slanted edge was used for DQE evaluation. This method uses beam stop as an edge to provide MTF characterization which is the basis for DQE. The following DQE calculation method was used [2].

$$DQE = 1 / (1 / DQE_{e-} + (1/DQE_{d}))$$

where $DQE_{e-} = MTF^2/NNPS$ is the dose independent part ($MTF = \text{Modulation Transfer Function}$, $NNPS = \text{Normalized Noise Power Spectrum}$) and $DQE_{d} = MTF^2 \text{conv}^2 Nq / DN^2$ is the dose dependent part ($DN = \text{dark noise}$, $\text{conv} = \text{conversion efficiency}$, $Nq = \text{dose rate in units e/px}$). The MTF is determined by the slanted edge method.

The DQE is analyzed for very low dose rates equal to 1e/p/frame which is the dose rate used for acquisition of SPA data.

SPA analysis with 3D particle reconstructions

Benchmark cryo-EM measurements using apoferritin demonstrates that Tundra Cryo-TEM can achieve sub-3Å resolution of the reconstructed 3D map. At this resolution, de novo protein structures can be determined, and important biological questions answered. The data was collected with pixel size of 0.75Å and processed and reconstructed using Relion SW. The data was collected using Thermo Scientific™ EPU™ software with pre-defined settings.

Tundra offers also new functionality in EPU that automatically checks and refines optical alignments and provides system status for high-quality data acquisition which was also used during acquisition. Furthermore, data quality was monitored on-the-fly using EPU quality monitor.

The complete SPA run was performed for different proteins to see the camera performance correlated to complexity of the protein structures.

RESULTS

More than ten CETA-F cameras were validated for image quality criteria at different HT to verify the performance of the product. The following figure (2) shows the DQE curve of the camera for most used HT. It is clearly visible that 100kV has the highest DQE at whole spatial frequency range.

Figure 2. DQE curve of CETA-F camera at different HT

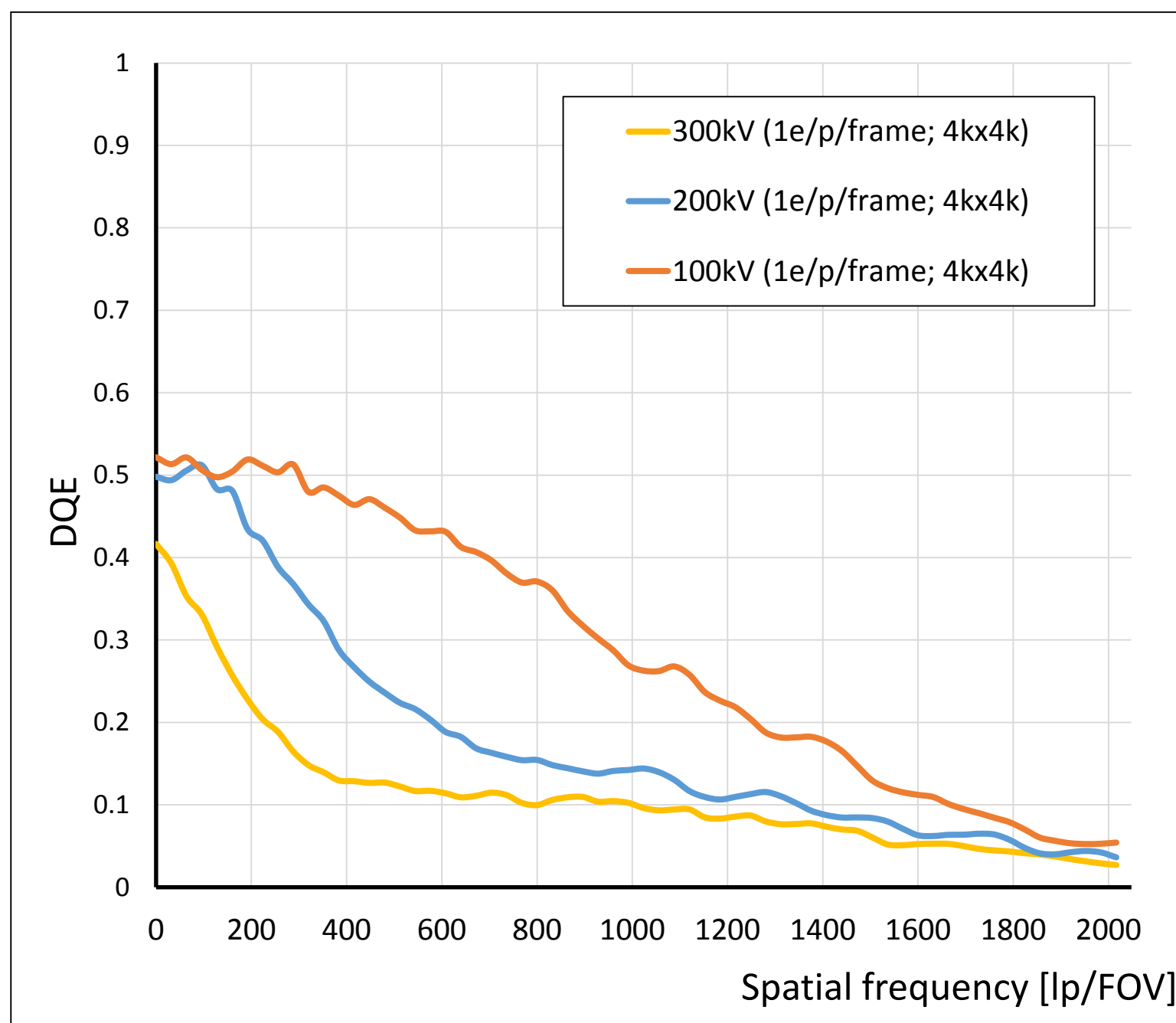
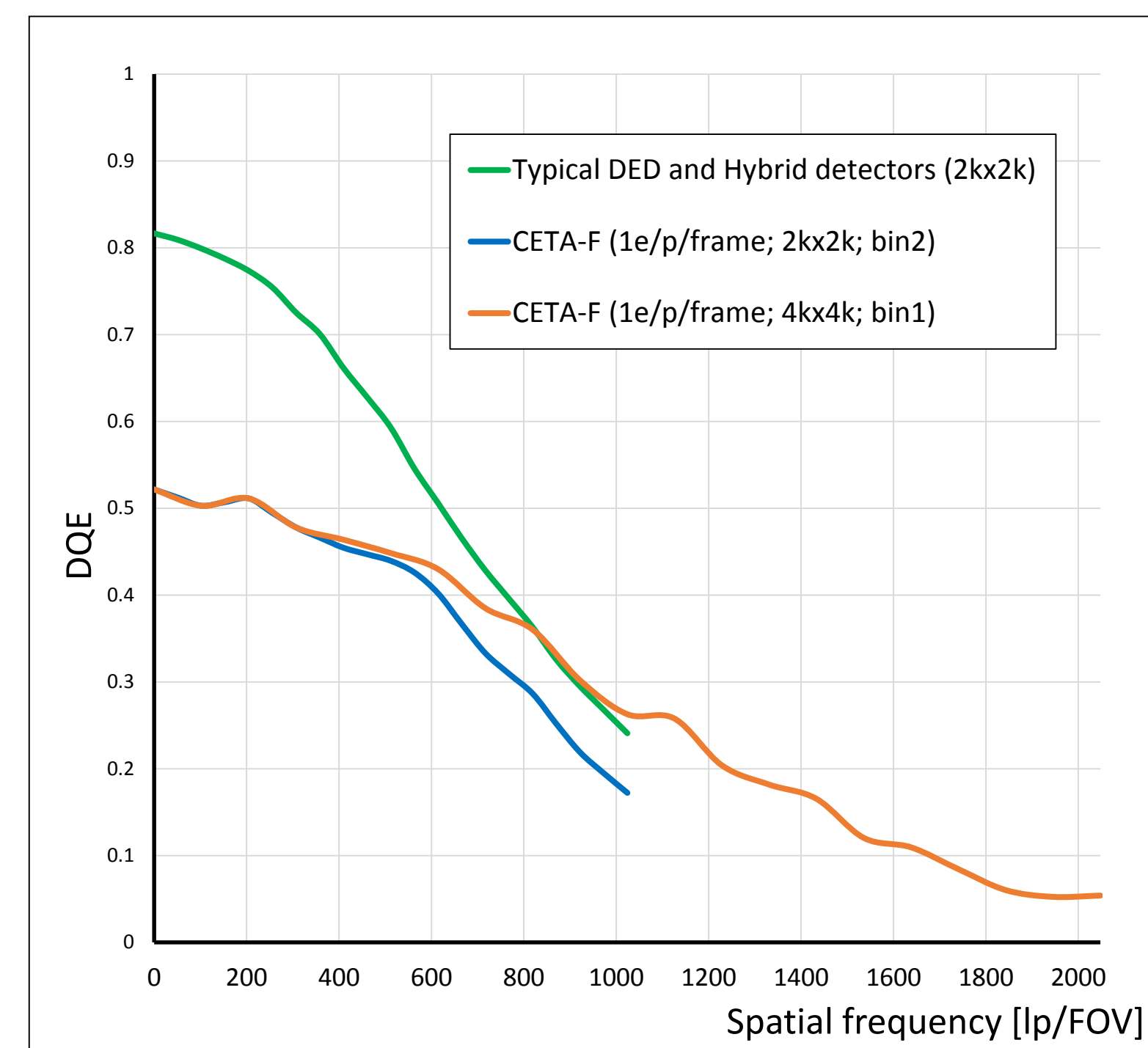


Figure 3 compares the CETA-F DQE at 100kV relative to the DQEs of DEDs (specifications for 100kV estimated) and hybrid detectors at 100kV. Since the pixel design of 100kV DED limits the camera to 2kx2k FOV the comparison is normalized to spatial frequency reachable by defined FOV.

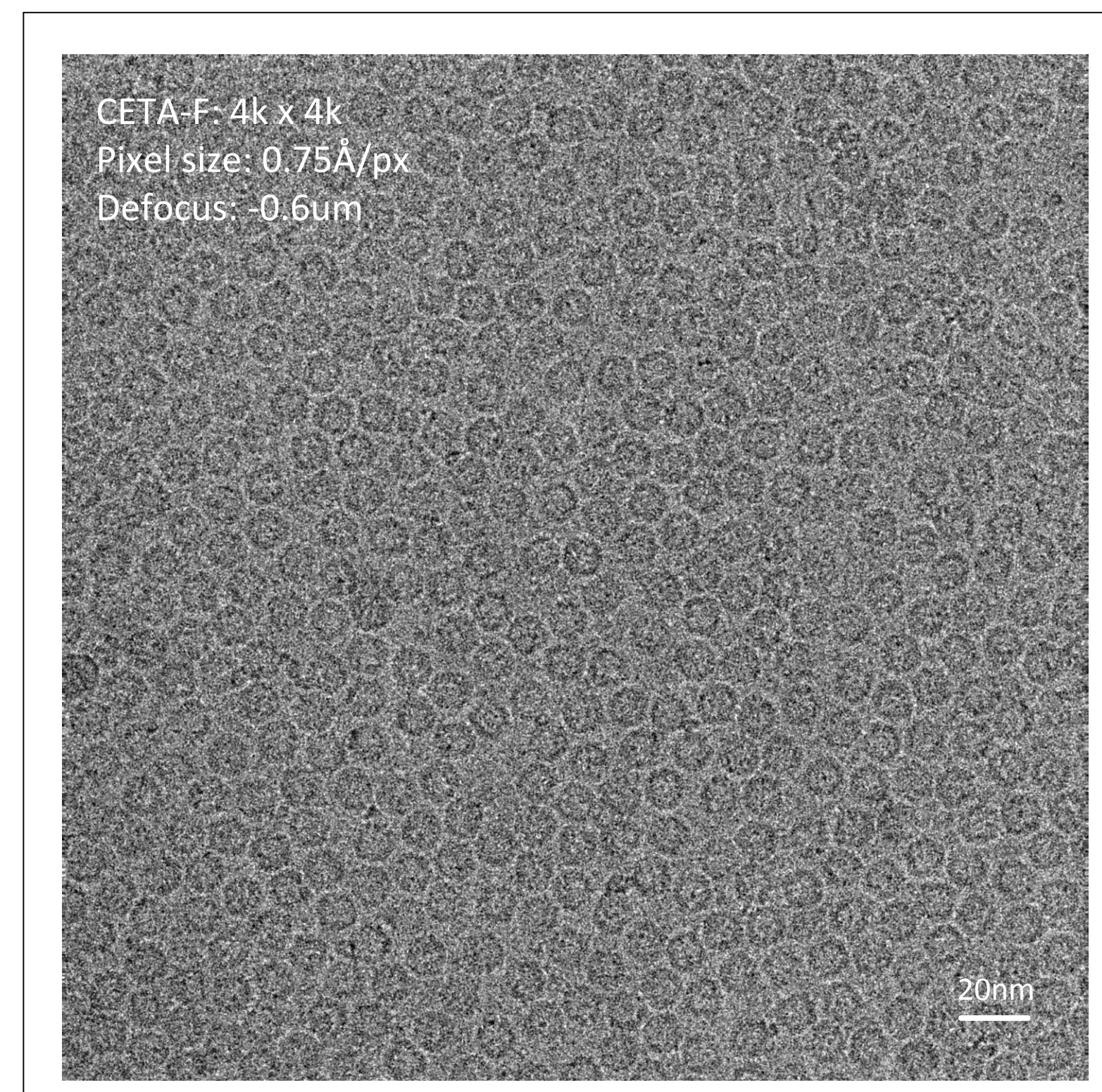
Figure 3 presents two CETA-F acquisition possibilities with differentiated by binning option. Full resolution (binning = 1) has higher spatial sampling and thus better high frequency DQE. Binning 2 option has advantage in storage capacity required for complete dataset. However, this option has lower DQE in higher spatial frequencies.

Figure 3. DQE comparison of multiple cameras @100kV



The single image from CETA-F as a composition of dose fractions optionally drift corrected for sample movement is shown in Figure 4 and Figure 5. Since the SNR is lower compared to DED or hybrid cameras the single image does not reach similar quality in contrast, however it is clearly visible that the particles can be easily recognized and separated. Figure 6 shows the 2D classes created from data acquisition. This figure illustrates how many details are present. The final 3D reconstruction of Apoferritin is visible in Figure 7.

Figure 4. CETA-F single image of Apoferritin



The following table provides an overview of performance of different camera concepts. Scintillator based camera has limitations in imaging performance at low dose, where signal does not cover all noise. However, this is proven as sufficient for biologically-relevant performance.

Table 1. Camera comparison

	CETA-F camera	Typical DED / Hybrid detectors
Resolution [pxs]:	4kx4k	up to 2kx2k
DQE @512lp/FOV:	>0.39	>0.55
Mode:	Linear	Counting

Figure 5. CETA-F single image of T20S proteasome

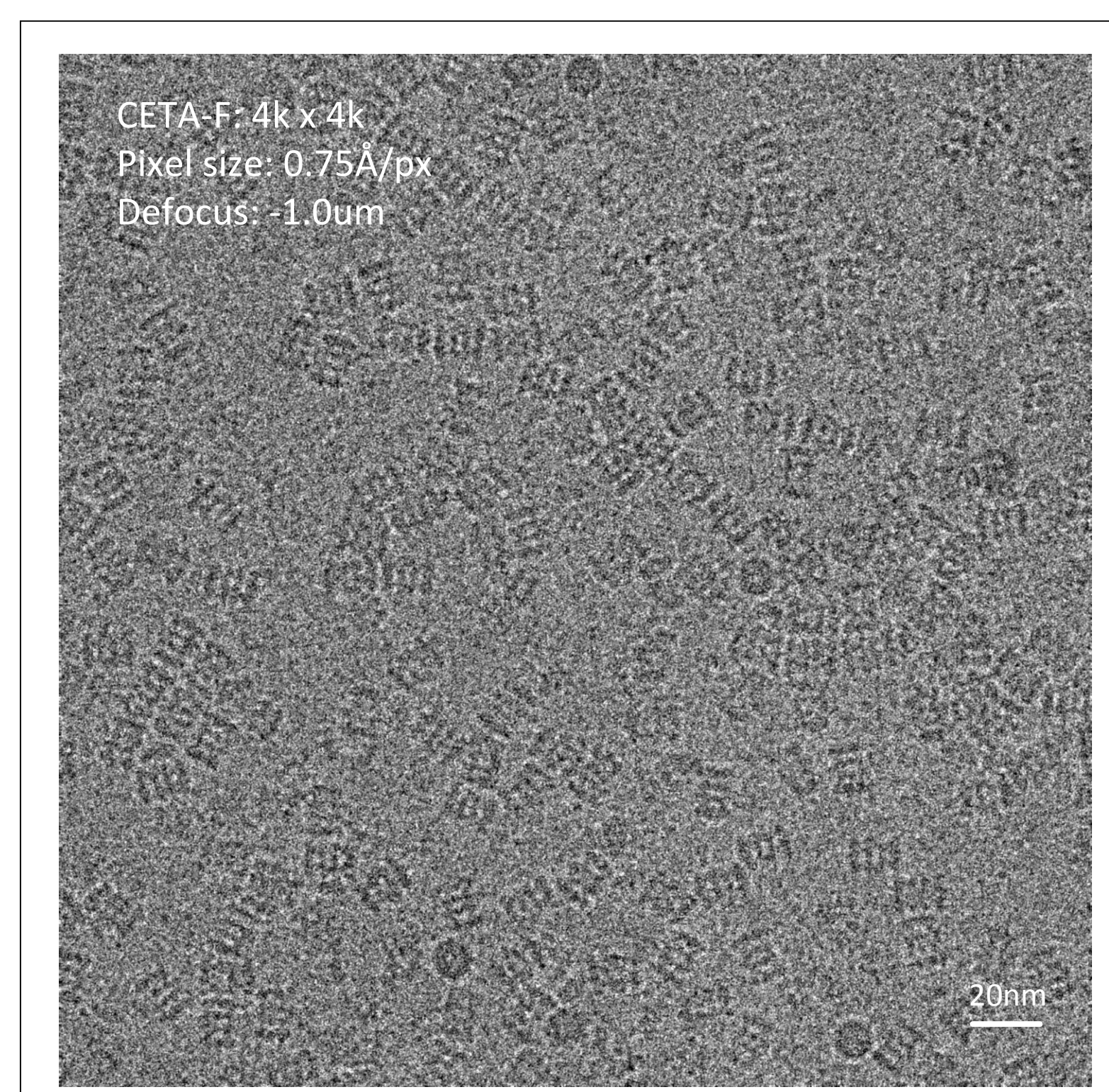


Figure 6. 2D classes of Apoferritin sample

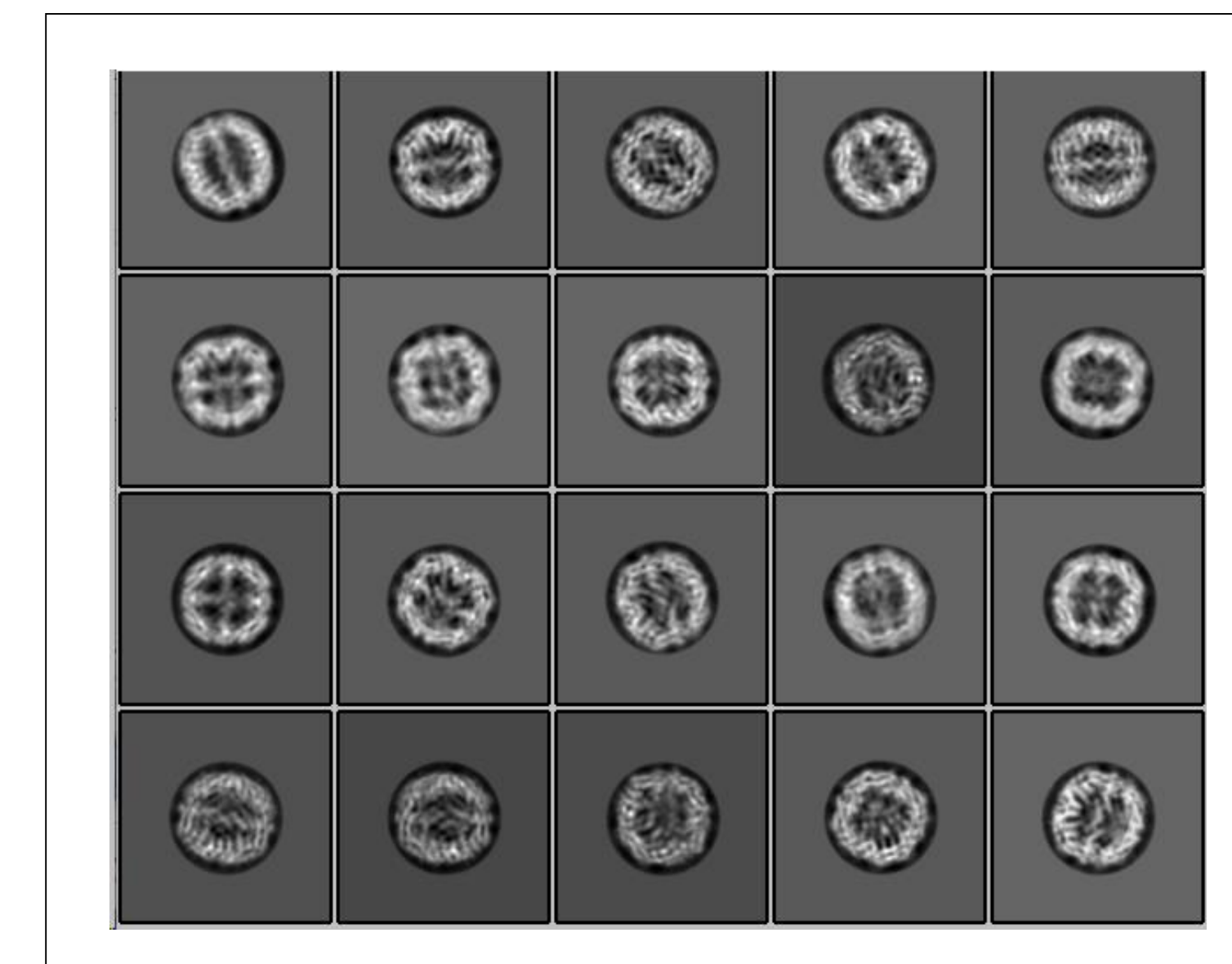
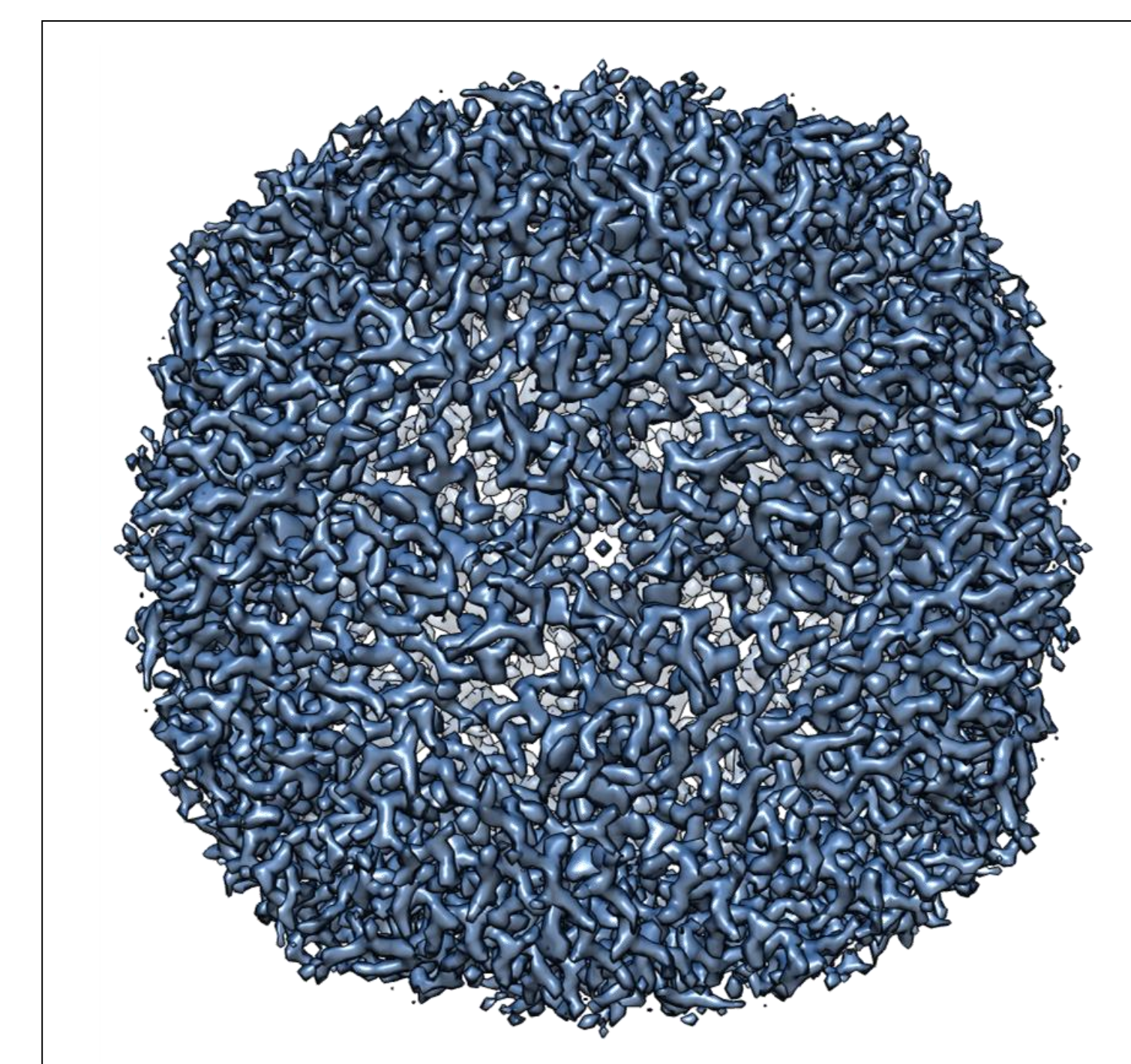


Figure 7. Apoferritin reconstruction at 2.6Å



CONCLUSIONS

Thermo Fisher Scientific introduced Tundra system at the end of last year. This system is equipped with scintillator-based camera which fulfills the goal to enable access of SPA technique in a cost optimized way. We demonstrated that using the scintillator-based CETA-F camera with an entry level 100kV SPA system provides a cost-effective solution with very good image quality, high FOV and radiation hardness.

We proved the system and camera quality with the performance comparison and most notably by a large number of sample reconstruction experiments. Latest Apoferritin (440kDa) sample experiment proved very good single image quality and 3D resolution of 2.6Å. The experiment with T20 proteasome proven 3D resolution of 3.0Å.

REFERENCES

- [1] K. Naydenova, G. McMullan, M.J. Peet, Y. Lee, P.C. Edwards, S. Chen, E. Leahy, S. Scotcher, R. Henderson and C.J. Russo, CryoEM at 100keV: a demonstration and prospects, IUCrJ. 2019 Nov 01; 6(Pt 6):1086-1098 <https://doi.org/10.1107/S2052252519012612>
- [2] M. Kuijper, G. van Hoften, B. Janssen, R. Geurink, S.D. Carlo, M. Vos, G. van Duinen, B. van Haeringen, M. Storms, FEI's direct electron detector developments: Embarking on a revolution in cryo-TEM, Journal of Structural Biology 192 (2015) 179–187
- [3] G. McMullan, S. Chen, R. Henderson, A.R. Faruqi, Detective quantum efficiency of electron area detectors in electron microscopy, Ultramicroscopy, Volume 109, Issue 9, August 2009, Pages 1126-1143, <https://doi.org/10.1016/j.ultramic.2009.04.002>

ThermoFisher
SCIENTIFIC